Surface Modification of Wood Fibers with Citric Acid as a Sustainable Approach to Develop Novel Polycaprolactone Based Composites for Packaging Applications

Laura Simonini * and Andrea Dorigato

Posted Date: 13 May 2025

doi: 10.20944/preprints202505.0930.v1

Keywords: citric acid; wood fibers; polycaprolactone; fiber/matrix adhesion; composites; packaging

 doi:10.20944/preprints202505.0930.v1

Article

Surface Modification of Wood Fibers with Citric Acid as a Sustainable Approach to Develop Novel Polycaprolactone Based Composites for Packaging Applications

Laura Simonini [1,2,*] and Andrea Dorigato [1,2]

[1] Department of Industrial Engineering, University of Trento, via Sommarive 9 38121 Trento (Italy)

[2] National Interuniversity Consortium of Materials Science and Technology (INSTM), via Giusti 9 50121 Florence (Italy)

* Correspondence: laura.simonini@unitn.it; +39 0461/283944

Abstract: In this work, novel biodegradable polycaprolactone (PCL) based composites for sustainable packaging applications were developed by adding surface-treated wood fibers (WFs). Specifically, WFs were treated with citric acid (CA) to improve the fiber/matrix adhesion and then melt compounded with PCL matrix. The presence of an absorption peak at 1720 cm^{-1} in the Fourier transform infrared (FTIR) spectra of CA-treated WFs, coupled with the increase in storage modulus and complex viscosity in the rheological analysis, confirmed the occurrence of the esterification reaction between CA and WFs, with a consequent increase in interfacial interaction with PCL matrix. Scanning electron microscopy (SEM) of the cryo-fractured surface of the composites highlighted that PCL was able to wet efficiently the fibers after CA treatment, with limited fiber pull-out. Quasi-static tensile tests showed that composites reinforced with CA-treated wood fibers exhibited a significant increase in yield strength (about 30% with a WF amount of 10% at 0 °C), and also a slight improvement in the VICAT softening temperature (about 6 °C with respect to neat PCL). Water absorption tests showed reduced water uptake in CA-treated composites, consistent with the reduced hydrophilicity confirmed by higher water contact angle values. Therefore, the results obtained in this work highlighted the potential of CA-treated WFs as reinforcement for PCL composites, contributing to the development of eco-sustainable and high-performance packaging materials.

Keywords: citric acid; wood fibers; polycaprolactone; fiber/matrix adhesion; composites; packaging

1. Introduction

In the last decades plastics revolutionized the packaging sector by extending the shelf life of fresh food, enabling essential health applications, contributing to lighter and safer shipping. However, the plastic materials used in packaging are usually petroleum-based polymers with a relatively high environmental impact, that can also contribute to the generation of polluting waste if not properly managed [1–5]. A possible solution to this problem could be the use of biocomposites made from biodegradable polymers and natural fibers [6–10]. Among the various biodegradable matrices, polycaprolactone (PCL) has emerged as a particularly promising candidate for packaging [11–16]. PCL is a biodegradable thermoplastic polyester known for its flexibility, excellent processability and biocompatibility [17–21]. Its low melting point (around 60 °C) makes PCL easy to process, enabling for energy-efficient manufacturing through extrusion, injection molding and thermoforming in a large scale perspective [22,23]. On the other hand, the limited melting temperature restricts its application where high heat resistance is required, especially at elevated humidity levels [24]. As a result, PCL is ideal for short-life uses such as food packaging and disposables [25]. Therefore, in order to enhance the properties of PCL and extend its applicability in

 doi:10.20944/preprints202505.0930.v1

the packaging sector, researchers have focused their attention on natural reinforcing fibers such as cotton [26], flax [27], hemp [28] and wood fibers [29].

Wood fibers (WFs), in particular, have been identified as an attractive option due to their abundance, renewability, biodegradability and low cost [30]. When incorporated into PCL, wood fibers can significantly improve the stiffness and the dimensional stability, thereby addressing some of the inherent limitations of this biopolymer matrix. For example, Cintra et al. co-extruded PCL with different contents (0, 5, and 15 wt%) of WFs, obtained as residues of the timber industry, investigating their thermo-mechanical properties [31]. Herrera et al. strongly improved the mechanical properties of thermoplastic biocomposites through PCL grafting inside holocellulose wood fibers [32]. Lo Re et al. produced PCL/WF biocomposites by introducing different concentrations of cellulose pulp fibers in a PCL matrix [33]. However, due to the difference in polarity between the hydrophobic PCL and the hydrophilic WFs, the successful integration of WFs into this polymer is not always efficient, leading often to poor interfacial bonding, fiber aggregation and reduced mechanical performance [34]. To overcome this problem, surface modification of the fibers is essential to improve their compatibility with the PCL [35–37].

An environmentally friendly and effective approach to treat wood fibers is the use of citric acid (CA), a natural organic acid that can be obtained from citrus fruits like lemons and limes or commercially produced through the fermentation of sugars by Aspergillus niger [38]. CA treatment has been shown to tailor the surface properties of wood fibers by increasing their surface roughness, improving hydrophobicity and introducing functional groups that promote a stronger interaction with biopolymer matrices [39]. Moreover, citric acid is non-toxic, biodegradable and derived from renewable sources, and it is therefore suitable for sustainable packaging solutions [40]. The idea behind this surface treatment is that the carboxyl (-COOH) groups of CA react with the hydroxyl (-OH) groups on WFs to form ester bonds (-COO-) and release water as a by-product, making the WFs surface more hydrophobic [39]. The reduction in -OH content on WFs surface could therefore improve the interfacial adhesion with the hydrophobic PCL matrix, leading to improved stress transfer and mechanical performance of the biocomposites. For example, Huang et al. treated cellulose fibers obtained from wheat straw with CA to improve their strength, due to the formation of a crosslinked structure [41]. Cui et al. modified the surface of cellulose with CA and used this functionalized filler as reinforcement in PLA based composites, achieving a better dispersion within the matrix and an increased interfacial adhesion [42]. However, although citric acid has been already investigated as a surface modifier for polysaccharide-based fibers, its specific application in the modification of wood fibers to improve compatibility with a PCL matrix has not so far been explored.

Therefore, the aim of this work was to explore, for the first time, the potential of novel PCL/WF biocomposites for sustainable packaging applications, obtained by modifying the surface of WFs using CA. Untreated and CA-treated WFs were characterized from a chemical, morphological and thermal point of view, and the resulting biocomposites were then analyzed in terms of their rheological, microstructural and thermo-mechanical properties. This comprehensive evaluation provided a deeper understanding of how CA surface modification could enhance the properties of PCL/WF biocomposites, contributing to the development of eco-sustainable and high-performance packaging materials.

2. Materials and Methods

2.1. Materials

PCL was supplied by Polysciences Inc. (Warrington, PA, USA) in 3 mm granules (density = 1.12 g/cm^3, molecular weight (M_w) = 50000 g/mol, glass transition temperature = -62 °C, melting temperature = 60 °C). Steico® Flex-036 wood fibers were supplied by Steico SE (Feldkirchen, Germany). They had an aspect ratio of 22-75 mm/mm and a bulk density of 60 kg/m^3. Citric acid monohydrate (CA) was supplied by Riedel-de Haën GmbH (Seelze, Germany) as a powder of 1 μm, with purity of 99.5 % and M_w of 210.14 g/mol. All the materials were used as received.

 doi:10.20944/preprints202505.0930.v1

2.2. Sample Preparation

Wood fibers (2 g) were soaked in 1 L of CA aqueous solution at different concentrations (0.05 M, 0.25 M, and 1.00 M) and stirred at 600 rpm for 1 hour at room temperature. Then, WFs were dried at 40 °C for 24 h under vacuum. These parameters were chosen from previous experiments of our group [39]. The chemical bonding between the CA and the WFs was achieved by thermally treating the fibers at 60, 80, 120 and 160 °C for 30 minutes. The treated fibers were then washed to neutral pH and dried at 40 °C for 24 h under vacuum. Figure 1 shows representative images of the treated WFs, where a gradual darkening in color is observed with increasing CA concentration and treatment temperature. This color change likely indicates a greater extent of chemical modification at elevated temperatures [39]. However, a temperature of 80 °C was chosen as the optimal one for the preparation of the treated fibers, as above this temperature the fibers appeared extremely brittle. The untreated wood fibers were indicated as WF, while CA treated fibers at 80 °C were designated as WF_5CA, WF_25CA and WF_100CA, in order to indicate the CA concentration in the aqueous solution (0.05 M, 0.25 M, and 1.00 M).

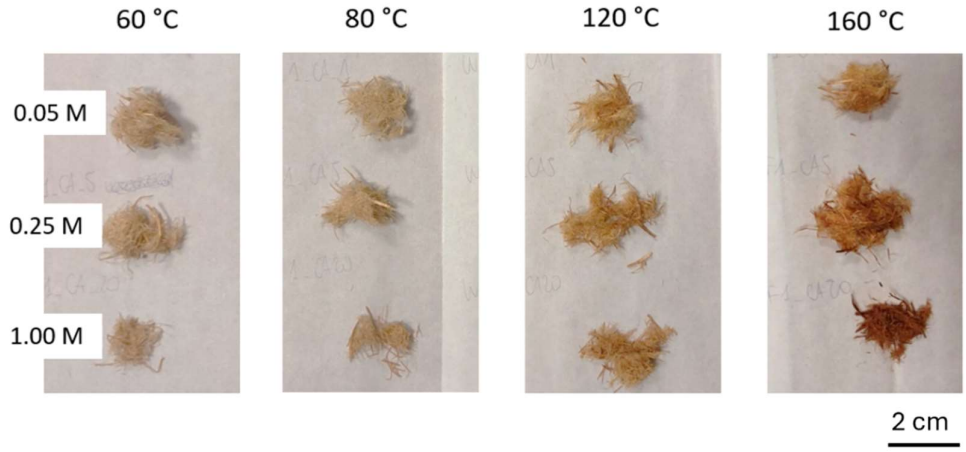

Figure 1. Representative image of wood fibers treated with CA at different concentrations and temperatures.

The preparation of PCL/WF biocomposites was achieved by melt compounding in a Thermo Haake® Reomix internal mixer (Thermo Fisher Scientific Inc., Waltham, MA, USA) at 80 °C for 9 minutes, setting a rotor speed of 50 rpm. The resulting compounds were then compression molded using a Carver 2699 hot press (Carverpress Inc., Wabash, IN, USA) at 80 °C for 6 minutes, applying a pressure of 2 MPa to produce 120×120×2 mm^3 samples. The list of the prepared formulations is reported in Table 1.

Table 1. List of prepared composites.

Sample	PCL content (%wt)	WF content (%wt)	CA solution (M)
PCL	100	0	-
PCL_5WF	95	5	-
PCL_10WF	90	10	-
PCL_20WF	80	20	-
PCL_10WF_5CA	90	10	0.05
PCL_10WF_25CA	90	10	0.25
PCL_10WF_100CA	90	10	1.00

 doi:10.20944/preprints202505.0930.v1

2.3. Experimental Techniques

2.3.1. Characterization of Wood Fibers

The chemical characterization of wood fibers was carried out by Fourier transform infrared spectroscopy (FTIR) in attenuated total reflectance mode using a Perkin Elmer Spectrum One FTIR spectrometer (Perkin Elmer Inc., Shelton, CT, USA). Four scans between 4000 and 650 cm^{-1}were performed for each sample, with a 4 cm^{-1} resolution.

The morphological features of WFs were investigated by using a Zeiss Supra 40 field-emission scanning electron microscope (FESEM) (Carl Zeiss AG, Oberkochen, Germany). Prior to the analysis, the samples were coated with a layer of a platinum/palladium (Pt/Pd) alloy (80:20) having a thickness of about 5 nm.

Thermogravimetric analysis (TGA) on wood fibers was carried out by using a Mettler TG50 thermobalance (Mettler Toledo Inc., Columbus, OH, USA) operating under a nitrogen flow of 100 mL/min in a temperature interval from 30 to 700 °C and at a heating rate of 10 °C/min. Therefore, it was possible to determine the temperature associated with a mass loss of 5 wt % ($T_{5\%}$), the degradation temperature (T_d) corresponding to the peak of the derivative thermogravimetric curve (DTG), and the residual mass after the test (m_{700}). One specimen was tested per composition.

2.3.2. Characterization of the Composites

The dynamic rheological properties of the composites were analyzed through a Discovery Hybrid Rheometer (DHR-2) (TA Instruments Inc., New Castle, DE, USA) by adopting a plate-plate configuration. Tests were carried out at 80 °C, applying a strain amplitude of 1% on circular specimens with a diameter of 25 mm, setting a gap between the plates of 1 mm. In this way, the trends of the storage modulus (G'), loss modulus (G''), loss tangent (tanδ) and complex viscosity (η) were investigated in an angular frequency (ω) range between 0.1 and 100 rad/s. Two specimens were tested for each composition.

The morphological characterization of cryo-fracture surface of the composites was carried out using a Zeiss Supra 40 field-emission scanning electron microscope (FESEM) (Carl Zeiss AG, Oberkochen, Germany). Prior to the analysis, the samples were coated with a platinum/palladium (Pt/Pd) alloy (80:20) coating having a thickness of about 5 nm.

The thermal properties of the composites were analyzed by differential scanning calorimetry (DSC) through a Mettler DSC30 calorimeter (Mettler Toledo Inc., Columbus, OH, USA). The samples were heated from -100 to 150 °C and subsequently cooled from 150 to -100 °C. Finally, a second heating stage was applied from -100 to 150 °C. These thermal ramps were performed at a rate of 10 °C/min, under a nitrogen flux equal to 100 mL/min. One specimen was tested for each composition. The relative degree of crystallinity (χ) of the PCL phase in the samples was calculated through Equation (1),

$$\boldsymbol{X} = \frac{\Delta \boldsymbol{H_m}}{\Delta \boldsymbol{H_{0m}} \cdot \boldsymbol{\varphi}} \qquad (1)$$

where ΔH_m is the enthalpy of fusion of PCL, φ is the weight fraction of PCL in the composite, and ΔH_{0m} is the standard melting enthalpy of the fully crystalline PCL, taken as 135.3 J/g [42]. Thermogravimetric analysis (TGA) on the composites was carried out by using a Mettler TG50 thermobalance (Mettler Toledo Inc., Columbus, OH, USA) under a nitrogen flow of 100 mL/min in a temperature interval from 30 to 700 °C at a heating rate of 10 °C/min. The tests allowed measuring the temperature associated with a mass loss of 5 wt % ($T_{5\%}$), the degradation temperature (T_d) corresponding to the peak of the derivative thermogravimetric curve (DTG), and the residual mass after the test (m_{700}). One specimen was tested per composition. Thermal diffusivity and thermal conductivity of the composites were measured at 20 °C through laser flash analysis (LFA) with a Netzsch LFA 447 instrument (Netzsch Gerätebau GmbH, Selb, Germany). Two circular specimens with a diameter of 12.7 mm and thickness 1 mm were tested for each composition.

 doi:10.20944/preprints202505.0930.v1

Quasi-static tensile properties of the composites were analyzed by using an Instron® 5969 universal testing machine (Instron Inc., Norwood, MA, USA), equipped with a load cell of 10 kN. 1BA type dumbbell specimens were tested according to the ISO 527 standard. Tests were carried out at 0 °C and 25 °C in order to simulate the use of packaging in refrigerated and room temperature conditions, respectively. The elastic modulus (E) was measured at a crosshead speed of 0.25 mm/min, imposing a maximum axial deformation level of 1%. The strain was recorded by using a dynamic extensometer Instron model 2620-601 (gauge length of 12.5 mm). According to ISO 527 standard, the elastic modulus was determined as a secant value between deformation levels of 0.05 % and 0.25 %. Tensile properties at break were evaluated at a crosshead speed of 100 mm/min, without using the extensometer. The yield stress (σ_y) and the elongation at break (ϵ_b) were determined. At least five specimens were tested for each composition. The Vicat softening temperature (VST) of the composites was determined according to ASTM D1525 standard. Tests were conducted at a heating rate of 120 °C/h using a HDT-Vicat tester model MP/3 (ATS Faar Industries Srl, Milano, Italy), applying a load of 50 N to rectangular specimens of 10x10x4 mm^3. At least three specimens were tested for each composition.

The water uptake (WU) capacity of the composites at room temperature was investigated by placing rectangular specimens of approximately 20×20×4 mm^3 in a container filled with 100 ml of water, and leaving them immersed for 90 days. At least three specimens per composition were tested. Mass variation due to water absorption was recorded over time after removing periodically the specimens from water. WU of the samples was calculated according to Equation (2)

$$\boldsymbol{WU = \frac{m_w - m_a}{m_a} \times 100} \quad (2)$$

where m_w is the mass of the specimens after being immersed in water, while m_a is the mass of the dry specimen. From water uptake tests the water diffusion coefficient (D) of the composites, described by Fick's law, was evaluated, as indicated in Equation (3)

$$\boldsymbol{D = \pi \left(S \cdot \frac{h}{4} \right)^2} \quad (3)$$

where h is the thickness of the sample and S is the ratio of the normalized mass uptake versus square root of time, as expressed in Equation (4)

$$\boldsymbol{S = \frac{M_t}{M_e \sqrt{t}}} \quad (4)$$

where M_t and M_e represent the mass of water absorbed at a given time (t) and at equilibrium condition (after 90 days), respectively.

Static contact angle measurements were conducted on square specimens 30x30x2 mm^3 using the sessile drop technique, by depositing at least five droplets of distilled water (volume = 2 ml) on the surface of the specimens. Images of the droplets were taken using a Thorlabs microscope (Thorlabs Inc., Newton, NJ, USA) and elaborated by ImageJ software (version 1.53a), in order to measure the contact angle (θ_c) values.

3. Results and Discussion

3.1. Characterization of Wood Fibers

3.1.1. Chemical and Microstructural Characterization of Wood Fibers

In Figure 2, the FTIR spectra of untreated and CA-treated WFs are shown.

 doi:10.20944/preprints202505.0930.v1

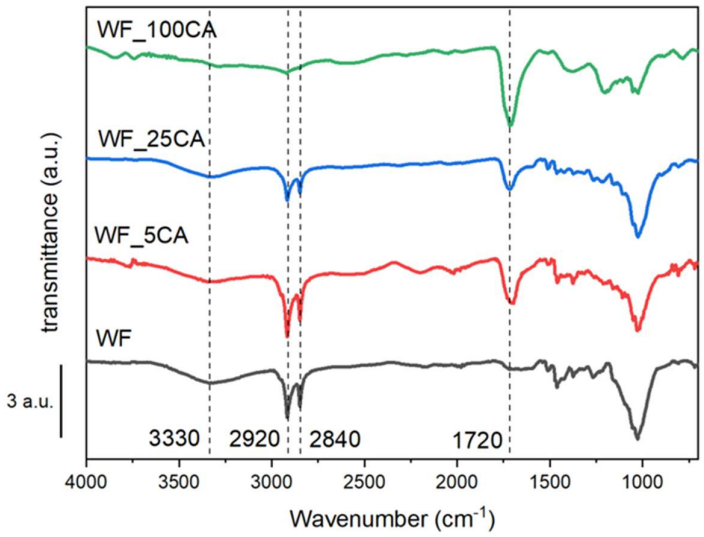

Figure 2. FTIR spectra of untreated and treated WFs with different CA concentrations.

Figure 2 shows the characteristic spectra of WFs, with absorption peaks associated to their constituents, i.e., cellulose, hemicellulose and lignin **[43]**. In particular, the broad peak at 3300 cm^{-1} corresponds to O-H stretching vibrations, due the hydroxyl groups naturally present on the fibers. The peaks at about 2900 cm^{-1} correspond to C-H stretching vibrations, while those around 1500 cm^{-1} are attributed to aromatic groups in lignin **[39]**. The presence of citric acid in the samples is demonstrated by the peak at 1720 cm^{-1}, whose intensity is proportional to the CA concentration. This peak is characteristic of C=O stretching vibrations, confirming the formation of ester bonds on the fiber surface. Moreover, increasing the CA concentration leads to more intense surface modification **[39]**. Correspondingly, the broad peak at 3300 cm^{-1} decreases in intensity in the treated WFs, particularly at elevated CA contents. This suggests that part of the hydroxyl groups on the surface of WFs have been consumed during the esterification reaction with CA.

In Figure 3, the SEM micrographs of untreated and CA-treated WFs are shown.

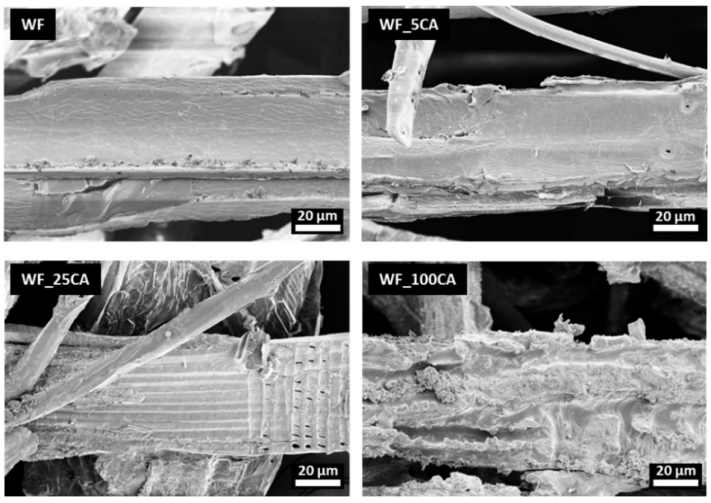

Figure 3. SEM micrographs of untreated and treated WFs at different CA concentrations.

It is evident that the surface morphology of the fibers is modified upon the CA treatment. Untreated WFs have a relatively smooth surface, while at low CA concentrations (WF_5CA) a slight roughening is observed, indicating a limited surface modification. At moderate CA contents (WF_25CA) etched regions become more visible, indicating a more intense treatment, while at the

 doi:10.20944/preprints202505.0930.v1

CA highest concentration (WF_100CA) there is a significant fibrillation, with the appearance of a very rough and fragmented surface, probably due to an extended esterification **[44]**. These chemical and morphological changes may improve the interfacial adhesion with the PCL matrix, with positive effects on the mechanical properties of the resulting composites.

3.1.2. Thermal Characterization of Wood Fibers

In Figure 4, the TGA thermograms and first derivative of mass loss of neat CA, untreated and CA-treated WFs are compared, while the most important results are summarized in Table 2.

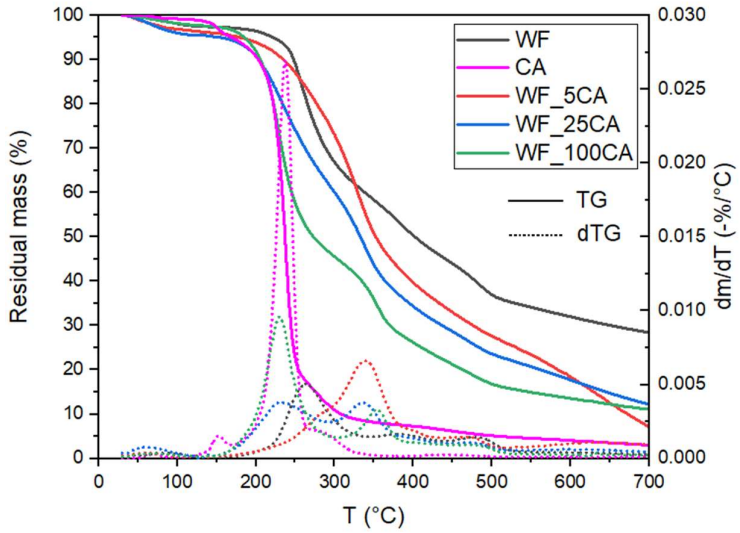

Figure 4. TGA thermograms of neat CA, untreated and CA-treated WFs.

Table 2. Results of TGA tests on neat CA, untreated and CA-treated WFs.

Samples	$T_{5\%}$ (°C)	$T_{d,CA}$ (°C)	T_{d,WF_1} (°C)	T_{d,WF_2} (°C)	T_{d,WF_3} (°C)	m_{700} (%)
WF	227.3	-	264.6	391.3	482.8	27.8
WF_5CA	190.4	-	256.3	338.3	479.3	7.5
WF_25CA	175.2	235.7	-	336.8	476.8	12.4
WF_100CA	182.3	225.5	-	355.5	477.2	11.2
CA	170.2	235.3	-	-	-	0.0

Figure 4 shows the differences in thermal degradation behaviour between untreated and CA-treated WFs. Untreated WF shows a multi-step degradation process, with $T_{5\%}$ of 227 °C, followed by three degradation stages at approximately 265 °C, 391 °C and 483 °C due to the thermal decomposition of cellulose, hemicellulose and lignin, respectively **[45]**. The residual mass at 700 °C is 27.8 %, indicating a significant char formation, typical of lignocellulosic materials. In contrast, neat CA decomposes rapidly, with a lower initial degradation temperature (170 °C), a single decomposition peak at 235 °C and no residue at 700 °C, indicating thus a complete volatilization at the end of the test **[46].** The treatment with CA significantly changes the thermal behaviour of the wood fibers. $T_{5\%}$ values for treated fibers (between 175 and 190 °C) are considerably lower than that of untreated WFs, indicating that the initial thermal stability of WF is negatively affected by the surface modification. Also the three degradation steps associated to WF constituents occur at lower temperatures (256 °C, 338 °C and 479 °C) compared to neat WFs, while the residual mass at 700 °C is reduced (up to 7.5% for the WF_100 CA). The position of the degradation peaks associated to wood

 doi:10.20944/preprints202505.0930.v1

constituents is not substantially affected by the CA content. However, even if the thermal stability of CA-treated fibers is generally lower than that of neat WFs, the thermal degradation resistance of these fibers is acceptable for their use in packaging, as their degradation can be detected at much higher temperatures than those required in service conditions.

3.2. Characterizaion of the Composites

3.2.1. Rheological Characterization of the Composites

The dynamic rheological properties of the composites are illustrated in Figures 5(a-d), where the trends of storage modulus (G′), loss modulus (G′′), loss tangent (tanδ) and complex viscosity (η) as a function of the frequency are respectively reported.

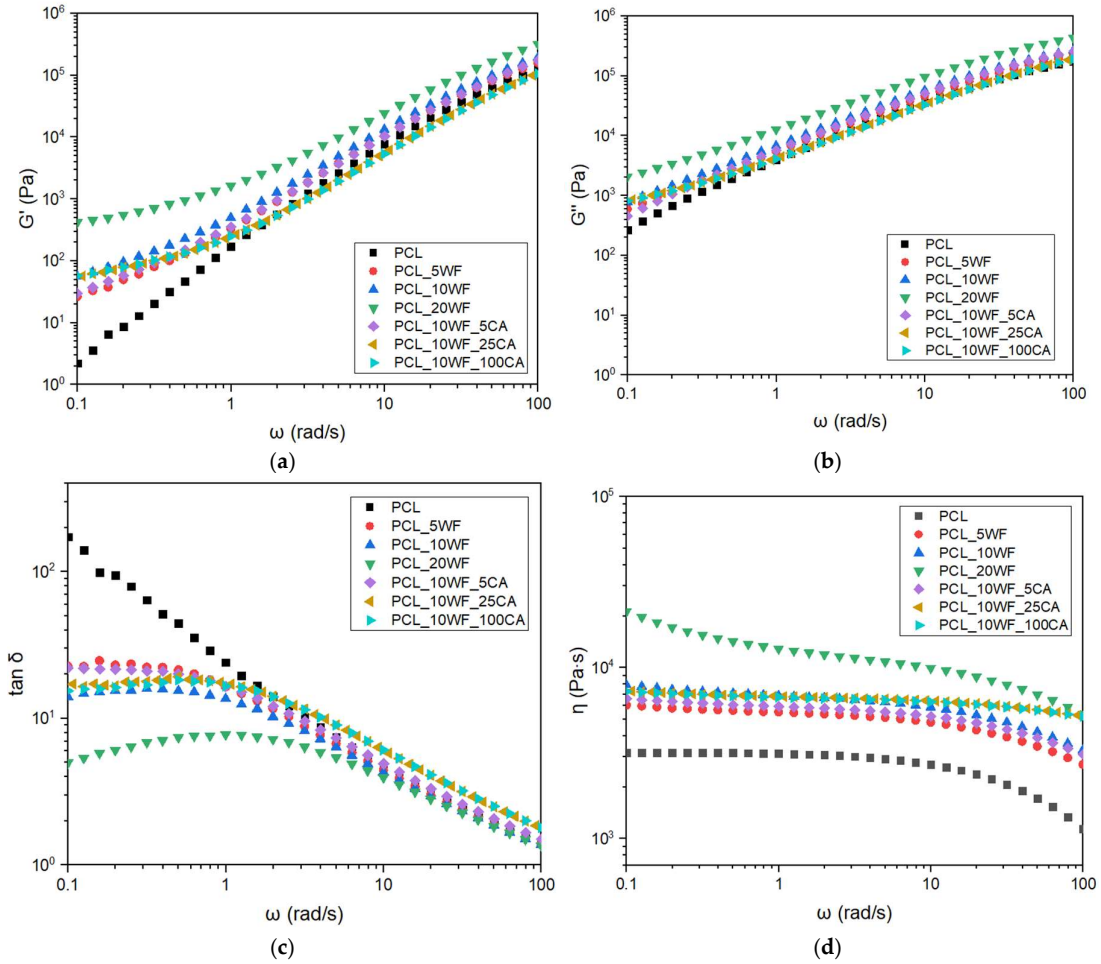

Figure 5. Dynamic rheological properties of PCL/WF composites. Trends of (a) storage modulus (G′), (b) loss modulus (G′′), (c) loss tangent (tanδ) and (d) complex viscosity (η) as a function of the angular frequency.

From Figure 5(a,b) it can be seen that both the storage modulus (G′) and the loss modulus (G′′) increase with the addition of WFs, especially in the low frequency regime, and this effect becomes more pronounced increasing the WF amount. The stiffening effect provided by the WF addition is confirmed by the corresponding decrease of the loss tangent values and the disappearance of the pseudoplastic plateau in the viscosity curve at low frequencies in Figure 5(c,d) **[47]**. On the other hand, while the incorporation of CA changes the chemical features and the morphology of WFs, its impact on the rheological properties of the composites is rather limited.

3.2.2. Morphological Characterization of Composites

 doi:10.20944/preprints202505.0930.v1

Figure 6(a-c) shows SEM micrographs of the cryo-fractured surface of the composites, while Figure 7(a,b) shows SEM images highlighting the fiber/matrix interfacial debonding in the axial and transverse direction (with respect to the embedded fibers).

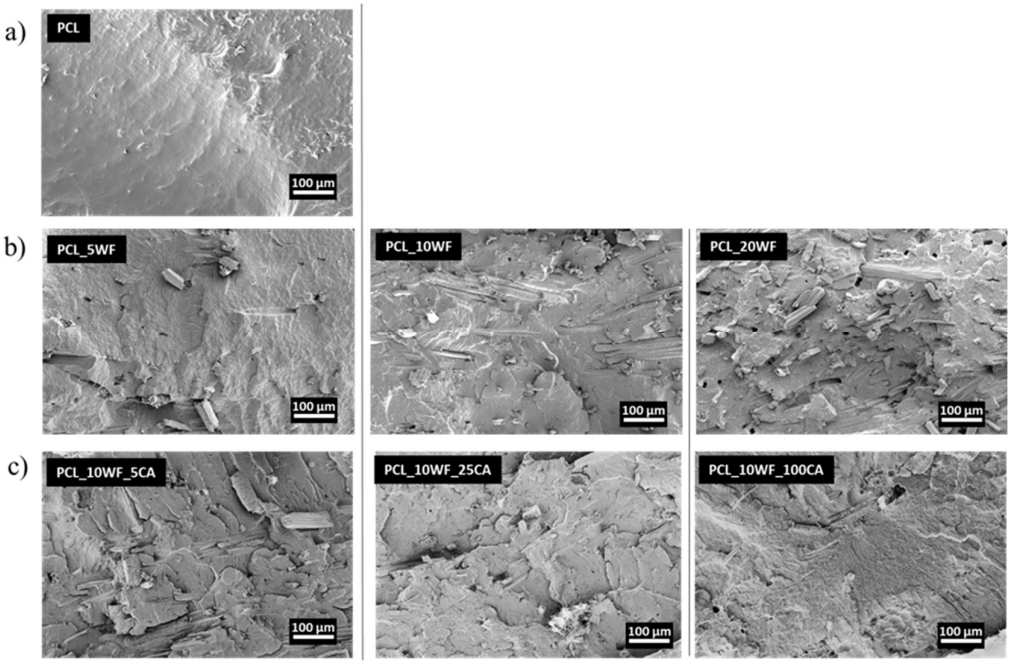

Figure 6. SEM micrographs of cryo-fractured surface of (a) PCL, (b) composites with increasing WF concentration and (c) composites containing 10 wt% of WF and increasing CA concentration.

 doi:10.20944/preprints202505.0930.v1

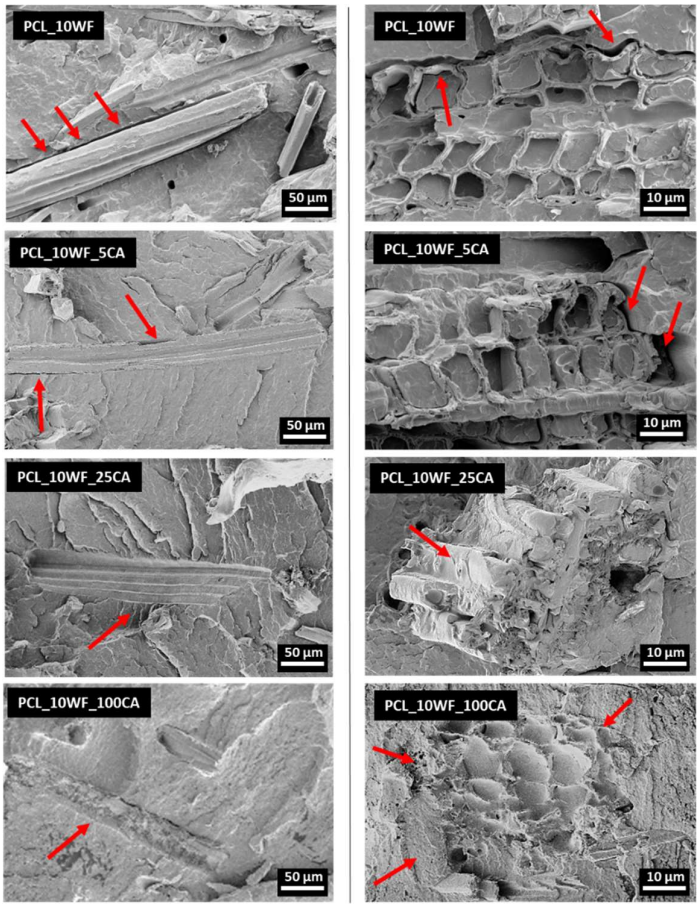

Figure 7. SEM micrographs showing fiber/matrix interfacial debonding in (a) axial and (b) transverse directions (with respect to the embedded WFs).

Neat PCL (Figure 6a) shows a relatively smooth surface with areas of extensive plastic deformation, indicative of a ductile fracture mechanism. As the WF content increases (Figure 6b), the fracture surface becomes rougher, with visible fiber pull-out and matrix deformation, suggesting a quite good stress transfer between the fibers and the polymer matrix, particularly for the PCL_20WF sample. As the CA content increases (Figure 6c), an even rougher fracture surface can be seen, indicating higher interfacial stress transfer and suggesting improved compatibility between the fibers and the PCL matrix.

In Figure 7a, the red arrows highlight the weak fiber/matrix interfacial adhesion in PCL_10 WF composite, showing areas where the fibers are completely debonded from the matrix. For PCL_10WF_5CA, some fiber pull-out and gaps between the fibers and the polymer matrix are still visible, indicating a moderate level of fiber/matrix interaction. For PCL_10WF_25CA composite the PCL matrix appears to wet better the fibers, probably due to esterification reaction obtained upon the CA treatment. In the PCL_10WF_100CA sample, the fracture surface appears smoother with less exposed fibers, indicating a stronger interfacial adhesion. Similar considerations can be made considering the SEM micrographs of the composites taken in the transversal direction (see Figure 7b).

3.2.3. Thermal Characterization of the Composites

DSC analysis revealed no significant differences in the thermal properties of the PCL phase, neither with the incorporation of wood fibers nor after their functionalization with CA. Therefore, these results have been reported in the Supplementary Material section (see Figure S1 and Table S1).

 doi:10.20944/preprints202505.0930.v1

Figure 8(a,b) shows the TGA thermograms and mass loss derivative curves of neat PCL and the relative composites, while the most significant results are summarized in Table 3.

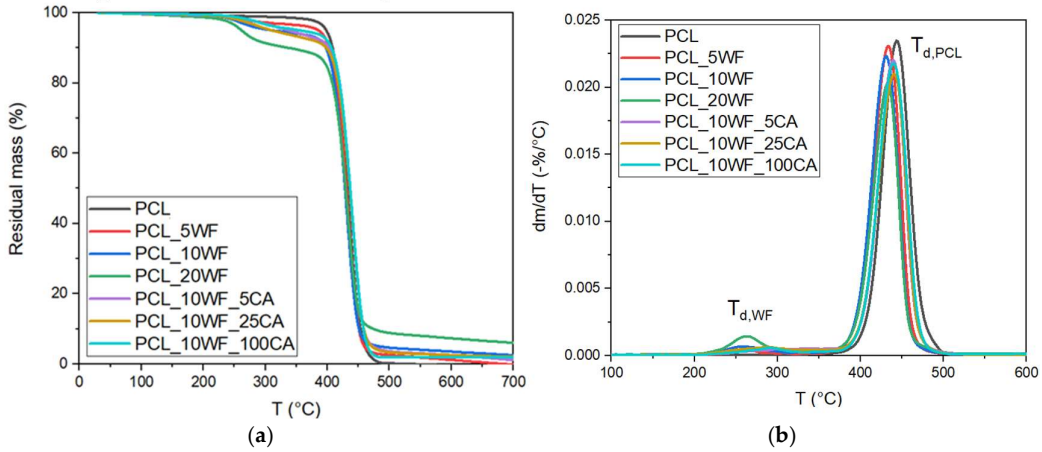

Figure 8. TGA thermograms of neat PCL and the relative composites. Trends of (a) residual mass and (b) mass loss derivative as a function of temperature.

Table 3. Results of TGA tests on neat PCL and the relative composites.

Samples	$T_{5\%}$ (°C)	$T_{d,WF}$ (°C)	$T_{d,PCL}$ (°C)	m_{700} (%)
PCL	398.2	-	433.5	0.0
PCL_5WF	386.5	259.0	433.3	0.0
PCL_10WF	321.2	258.0	432.3	2.5
PCL_20WF	259.2	260.5	431.2	6.0
PCL_10WF_5CA	334.3	284.7	438.5	1.1
PCL_10WF_25CA	314.1	296.2	437.5	1.9
PCL_10WF_100CA	321.2	298.7	437.7	2.0

The $T_{5\%}$ of neat PCL is observed at 398 °C, which strongly decreases with the addition of WFs reaching 259 °C for the PCL_20WF sample. This decrease can be attributed to the presence of the lignocellulosic fibers, which typically degrade at lower temperatures than the PCL matrix (433 °C). In fact, $T_{d,WF}$ corresponds to the degradation of WFs in the composites and its values are observed approximately between 258 °C and 298 °C. On the other hand, the presence of CA does not significantly alter the value of T5% but strongly increases the value of Td,WF compared to the PCL_10WF sample, contrary to what is seen in Table 2. This apparent discrepancy can be explained by considering that, although CA-treated fibers are generally rougher and more fibrillated that can promote earlier thermal degradation, their incorporation into the PCL matrix change the thermal behavior. Once embedded, the reduced availability of surface hydroxyl groups due to esterification with CA may play a protective role, limiting their thermal degradation. **[39]**.

The degradation of PCL ($T_{d,PCL}$) is observed at 433 °C and is not substantially affected by the WF content. However, CA treatment slightly shifts $T_{d,PCL}$ to higher temperatures, with PCL_10WF_100CA reaching 437 °C. The residual mass at 700 °C increases with the PCL content up to 6.0% mass in the case of PCL_20WF, due to carbonaceous residues from the decomposition of the WFs, and it is not substantially affected by the CA functionalization. Generally speaking, all the prepared composites maintain a good thermal stability well above 200 °C, and are therefore suitable for packaging applications.

Results from LFA analysis are reported in the Supplementary material section. In Figure S2(a,b) the values of thermal diffusivity and thermal conductivity of the investigated composites are

 doi:10.20944/preprints202505.0930.v1

reported. It is evident that the introduction of WFs and the CA treatment do not significant affect the thermal diffusivity and the thermal conductivity of the composites.

3.2.4. Mechanical Characterization of Composites

In Figure 9(a,b) representative stress-strain curves from quasi-static tensile tests on neat PCL and the relative composites at 0 °C and 25 °C are shown, while the values of elastic modulus (E), stress at yield (σ_y) and elongation at break (ϵ_b) are summarized in Table 4, together with the Vicat softening temperature (VST) obtained from Vicat tests.

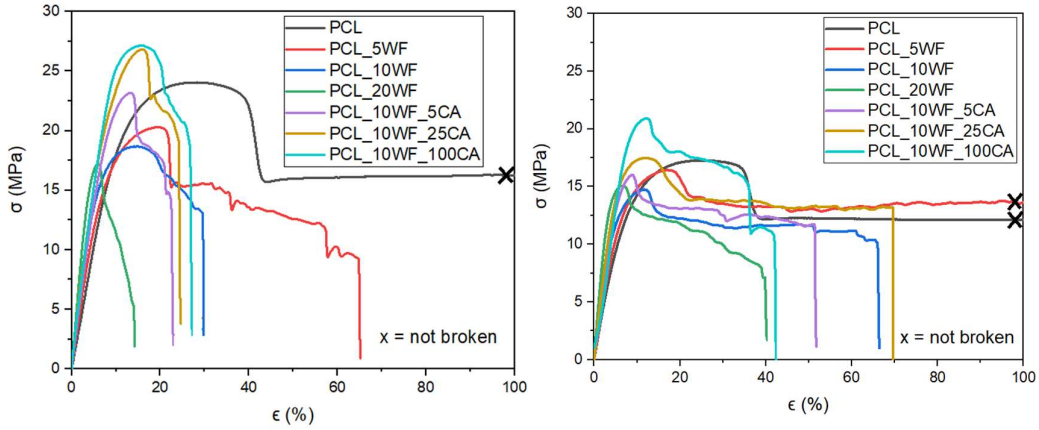

Figure 9. Representative stress-strain curves from quasi-static tensile tests on neat PCL and the relative composites at (a) 0 °C and (b) 25 °C.

Table 4. Results from quasi-static tensile tests at 0 °C and 25 °C and Vicat grade of neat PCL and the relative composites.

Sample	0 °C			25 °C			VST
	E (MPa)	σ_y (MPa)	ϵ_b (%)	E (MPa)	σ_y (MPa)	ϵ_b (%)	(°C)
PCL	228 ± 14	23 ± 1	358 ± 83	202 ± 5	17 ± 1	1301 ± 4	52.7 ± 0.6
PCL_5WF	259 ± 16	19 ± 1	46 ± 19	271 ± 15	14 ± 3	1016 ± 50	54.2 ± 0.5
PCL_10WF	327 ± 14	19 ± 1	27 ± 10	333 ± 3	15 ± 1	61 ± 21	56.1 ± 0.5
PCL_20WF	458 ± 15	17 ± 1	14 ± 1	467 ± 69	14 ± 1	36 ± 11	58.8 ± 0.7
PCL_10WF_5CA	337 ± 30	23 ± 1	23 ± 2	337 ± 37	14 ± 2	49 ± 10	56.5 ± 0.3
PCL_10WF_25CA	354 ± 27	27 ± 2	33 ± 7	348 ± 31	15 ± 2	54 ± 19	57.7 ± 0.5
PCL_10WF_100CA	354 ± 31	26 ± 3	27 ± 2	348 ± 21	19 ± 3	53 ± 22	58.8 ± 0.5

As it could be expected, the addition of WFs significantly increases the elastic modulus, up to 100% at 0 °C and 131% at 25 °C in case of PCL_20WF composite. On the other hand, the presence of untreated WFs reduces the yield strength of PCL. This reduction (up to 30% at 0 °C and 18% at 25 °C for PCL_20WF) is indicative of rather weak interfacial fiber/matrix adhesion. Interestingly, the CA treatment slightly increases the elastic modulus but leads to an evident enhancement in yield strength (up to 30% at 0 °C and 21% at 25 °C for PCL_10WF_100CA compared to PCL_10WF). This improvement can be attributed to an enhanced interfacial adhesion between the WFs and the PCL matrix due to esterification reaction on WFs surface provided by CA. As it could be expected, the elongation at break generally shows a significant decrease with wood fiber addition, especially at

 doi:10.20944/preprints202505.0930.v1

higher WF contents (14% at 0 °C and 36% at 25 °C for the PCL_20WF composite), without any significant effect of the CA treatment.

PCL has the lowest VST at 52.7 °C, indicating its relatively low dimensional stability approaching the melting temperature. Accordingly to elastic modulus results, the incorporation of WFs leads to a gradual increase in VST, with PCL_20WF reaching the highest value (58.8 °C). This trend suggests that the presence of WFs limits the mobility of the PCL macromolecules, thus increasing the dimensional stability. CA treated composites show a slight increase in VST compared to the untreated PCL_10WF (56.1 °C). In fact, PCL_10WF_5CA shows a VST of 56.5 °C, while PCL_10WF_100CA reaches 58.8 °C. Once again, this improvement can be attributed to the enhanced interfacial adhesion between the WFs and the PCL matrix **[48]**.

3.2.5. Water Uptake and Contact Angle Mesurements

Figure 10 shows the water absorption curves of neat PCL and the relative composites as a function of time, while the diffusion coefficient (D) and the values of water uptake after 90 days (WU_{90}) are summarized in Table 5.

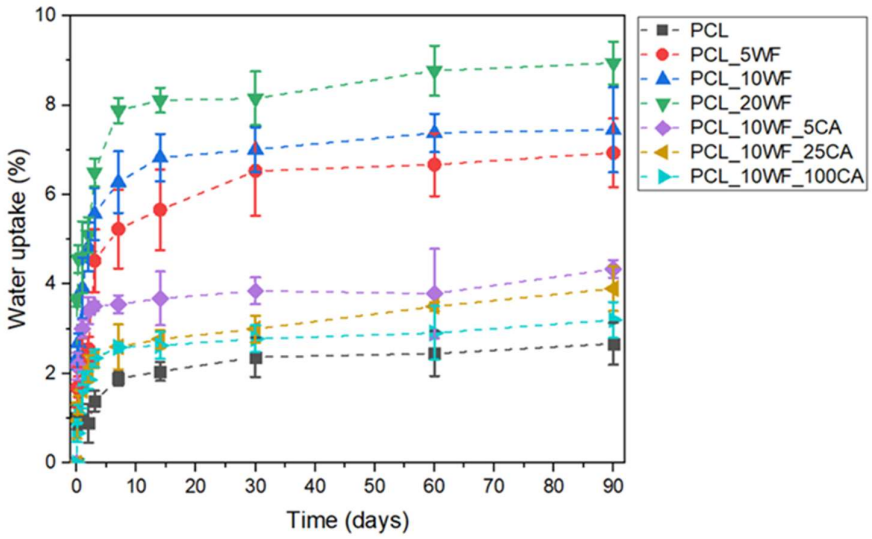

Figure 10. Water absorption curves at 23 °C of neat PCL and the relative composites.

Table 5. Results from water uptake tests at 23 °C on neat PCL and the relative composites.

Samples	D (10^{-13} × m²/s)	WU_{90} (%)
PCL	1.06 ± 0.36	2.67 ± 0.47
PCL_5WF	1.31 ± 0.46	6.93 ± 0.77
PCL_10WF	1.27 ± 0.52	7.44 ± 0.95
PCL_20WF	1.27 ± 0.64	8.94 ± 0.48
PCL_10WF_5CA	1.22 ± 0.43	4.34 ± 0.20
PCL_10WF_25CA	1.18 ± 0.36	3.90 ± 0.51
PCL_10WF_100CA	1.19 ± 0.62	3.22 ± 0.42

Neat PCL has a diffusion coefficient of 1.06×10^{-13} m²/s and a water absorption of 2.67% after 90 days, and these results are comparable to those found in the literature **[49]**. The introduction of WFs increases both the diffusion coefficient and water absorption tendency, as expected due to the hydrophilic nature of lignocellulosic fibers. For example, the diffusion coefficient of PCL_10WF is 1.27×10^{-13} m²/s and the water absorption value after 90 days is 7.44%. This increase is even more pronounced for PCL_20WF composite, with the highest WU90 value (8.94%) due to the higher

 doi:10.20944/preprints202505.0930.v1

amount of WFs **[50]**. On the other hand, the functionalization of WF with CA results in a reduction of both D and WU_{90} values. For example, PCL_10WF_100CA has a diffusion coefficient of 1.19×10^{-13} m^2/s and water uptake value after 90 days of 3.22 %. This means that the esterification reaction between CA and WF has effectively reduced the number of available hydroxyl groups on WFs surface limiting the uptake of water **[51]**. Therefore, while the incorporation of untreated WFs increases the water absorption tendency of the resulting composites, the chemical modification of the fibers through CA can mitigate this effect, making CA-treated WFs/PCL composites more suitable for packaging applications, where hydrophobicity and enhanced water resistance is generally required.

Contact angle measurements provide information about the surface properties and the wettability of the samples. Figure 11 shows the image of single droplets of water deposited on the surface of samples, while in Table 6 the values of static contact angles are summarized.

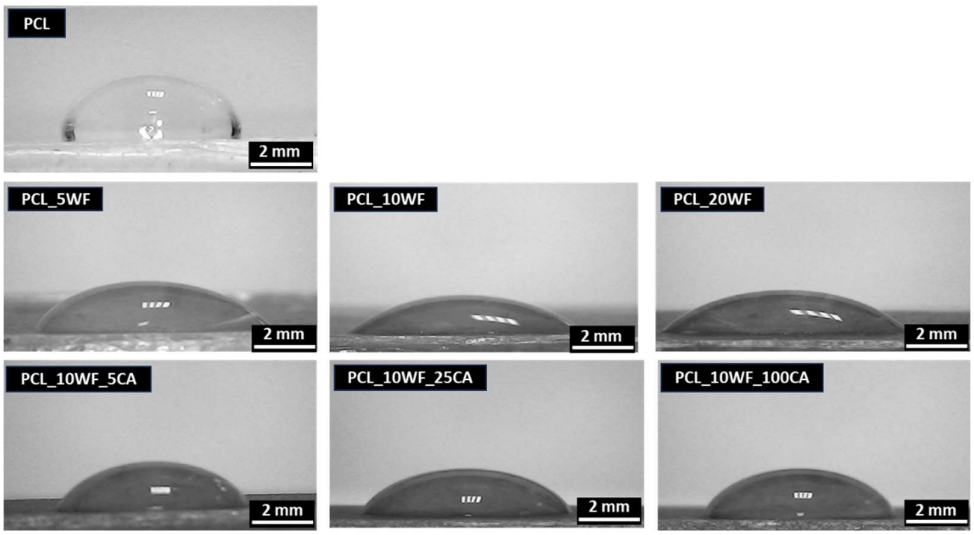

Figure 11. Representative images of static contact angle measurements on neat PCL and the relative composites.

Table 6. Static contact angle values of neat PCL and the relative composites.

Samples	θ_c (°)
PCL	84.2 ± 3.1
PCL_5WF	47.8 ± 2.9
PCL_10WF	51.2 ± 2.4
PCL_20WF	45.4 ± 4.5
PCL_10WF_5CA	55.2 ± 3.4
PCL_10WF_25CA	56.5 ± 1.3
PCL_10WF_100CA	61.2 ± 2.3

The contact angle measurements indicate significant changes in the wettability of the composites due to the incorporation of WFs and the addition of CA. Neat PCL exhibits the highest contact angle (84.2°), demonstrating its inherent hydrophobicity **[52]**. However, the introduction of WFs drastically reduces the contact angle (e.g., 47.8° for PCL_5WF and 45.4° for PCL_20WF), indicating an increased hydrophilicity. This behaviour could be expected, due to the presence of hydroxyl group on the surface of WFs, which increase water affinity **[53]**. CA functionalization modifies the surface properties, leading to an increase in contact angle compared to untreated WF composites. In fact, PCL_10WF_5CA (55.2°), PCL_10WF_25CA (56.5°) and PCL_10WF_100CA (61.2°) exhibit higher contact angles than PCL_10WF (51.2°). This suggests that CA treatment, by enhancing interfacial

 doi:10.20944/preprints202505.0930.v1

bonding between PCL and WF through esterification reactions and reducing the number of available hydroxyl groups on the WF surface, reduces the hydrophilicity and the wettability of the composites. This can be considered as a positive aspect in view of the future application of these materials in packaging.

4. Conclusions

In this work, novel biodegradable polycaprolactone (PCL) composites for sustainable packaging applications were developed by adding surface-treated wood fibers (WF). Specifically, WFs were treated with citric acid (CA) to improve their adhesion with the polymeric matrix. The surface modification of WFs with CA was first evaluated by a comprehensive fiber characterization. Fourier transform infrared (FTIR) spectroscopy confirmed the occurrence of esterification reactions between CA and the fiber surface, evidenced by a characteristic absorption peak at 1720 cm^{-1} having intensity proportional to the CA content. Scanning electron microscopy (SEM) of the treated fibers showed increased surface roughness and fibrillation, which might improve the mechanical interlocking with the polymer matrix and thus the interfacial adhesion. Thermogravimetric analysis (TGA) showed a slight reduction in thermal stability for CA-treated fibers due to increased surface reactivity after treatment. The fibers were then melt compounded with PCL matrix to obtain composites that were characterized in terms of their rheological, morphological, and thermo-mechanical properties. The rheological properties of composites were only slightly affected by CA treatment, with small increases in storage modulus and complex viscosity. SEM analysis of the cryo-fractured surfaces of the composites highlighted an enhanced fiber/matrix interfacial adhesion in the CA-treated WF filled compositess, with less fiber pull-out. Tensile tests showed a significant increase in yield strength (over 30% at 0°C and 21% at 25°C for the PCL_10WF_100CA sample with respect to PCL_10WF), and also VICAT softening temperature was slightly enhanced (about 6 °C with respect to neat PCL). In addition, water absorption tests and contact angle measurements demonstrated reduced water uptake and hydrophilicity in the CA-treated WF filled composites. Therefore, the results obtained in this work highlighted the potential of CA-treated WFs as reinforcement for PCL composites, contributing to the development of novel eco-sustainable and high-performance packaging materials.

Supplementary Materials: The following supporting information can be downloaded at the website of this paper posted on Preprints.org, *Figure S1*: DSC thermograms of neat PCL and the relative composites. (a) First heating, (b) cooling and (c) second heating; *Table S1*: Results of DSC tests on neat PCL and the relative composites; *Figure S2:* Results of (a) thermal diffusivity and (b) thermal conductivity of the neat PCL and the relative composites, obtained through Laser Flash Analysis.

Author Contributions: Conceptualization, L.S. and A.D.; methodology, L.S. and A.D.; validation, L.S. and A.D.; formal analysis, L.S. and A.D.; investigation, L.S.; data curation, L.S.; writing—original draft preparation, L.S.; writing—review and editing, L.S and A.D.; visualization, L.S and A.D.; supervision, A.D. All authors have read and agreed to the published version of the manuscript.

Data Availability Statement: Data are available on request.

Conflicts of Interest: The authors declare no conflicts of interest.

References

1. Ncube, L.; Ude, A.; Ogunmuyiwa, E.; Zulkifli, R.; Beas, I. An overview of plastic waste generation and management in food packaging industries. *Recycling* **2021**, *12*, 12-37.
2. Muhib, M.; Uddin, M.; Rahman, M.; Malafaia, G. Occurrence of microplastics in tap and bottled water, and food packaging: A narrative review on current knowledge. *Science of The Total Environment* **2023**, *865*, 161274-161285.
3. Tas, C.; Unal, H. Thermally buffering polyethylene/halloysite/phase change material nanocomposite packaging films for cold storage of foods. *Journal of Food Engineering* **2021**, *292*, 110351-110359.

 doi:10.20944/preprints202505.0930.v1

4. Antonopoulos, I.; Faraca, G.; Tonini, D. Recycling of post-consumer plastic packaging waste in the EU: Recovery rates, material flows, and barriers. *Waste Management* **2021**, *126*, 694-705.
5. Simonini, L.; Sorze, A.; Maddalena, L.; Carosio, F.; Dorigato, A. Mechanical reprocessing of polyurethane and phenolic foams to increase the sustainability of thermal insulation materials. *Polymer Testing* **2024**, *8*.
6. Souza, V.; Pires, J.; Rodrigues, C.; Coelhoso, I.; Fernando, A. Chitosan composites in packaging industry - current trends and future challenges. *Polymers* **2020**, *11*, 417-487.
7. Amara, C.; El Mahdi, A.; Medimagh, R.; Khwaldia, K. Nanocellulose-based composites for packaging applications. *Current Opinion in Green and Sustainable Chemistry* **2021**, *31*, 100512-100527.
8. Deng, J.; Zhu, E.; Xu, G.; Naik, N.; Murugadoss, V.; Ma, M.; Guo, Z.; Shi, Z. Overview of renewable polysaccharide-based composites for biodegradable food packaging applications. *Green Chemistry* **2022**, *24*, 480-492.
9. Stark, N.; Matuana, L. Trends in sustainable biobased packaging materials: A mini review. *Materials today sustainability* **2021**, *15*, 100084-100093.
10. Cazón, P.; Vázquez, M. Bacterial cellulose as a biodegradable food packaging material: A review. *Food Hydrocolloids* **2021**, *113*, 106530-106539.
11. Thakur, M.; Majid, I.; Hussain, S.; Nanda, V. Poly (ε-caprolactone): A potential polymer for biodegradable food packaging applications. *Packaging Technology and Science* **2021**, *34*, 449-461.
12. Diken, M.; Kocer Kizilduman, B.; Doğan, S.; Doğan, M. Antibacterial and antioxidant phenolic compounds loaded PCL biocomposites for active food packaging application. *Journal of Applied Polymer Science* **2022**, *139*, 52423-52438.
13. Amini, E.; Valls, C.; Roncero, M. Promising nanocomposites for food packaging based on cellulose–PCL films reinforced by using ZnO nanoparticles in an ionic liquid. *Industrial Crops and Products* **2023**, *193*, 116246-116257.
14. Gutiérrez, T.; Mendieta, J.; Ortega-Toro, R. In-depth study from gluten/PCL-based food packaging films obtained under reactive extrusion conditions using chrome octanoate as a potential food grade catalyst. *Food Hydrocolloids* **2021**, *111*, 106255-106270.
15. Gürler, N.; Pekdemir, M.; Torğut, G.; Kök, M. Binary PCL–waste photopolymer blends for biodegradable food packaging applications. . *Journal of Molecular Structure* **2023**, *1279*, 134990-134997.
16. Khan, S.; Dhakal, H.; Saifullah, A.; Z, Z. Improved Mechanical and Thermal Properties of Date Palm Microfiber-Reinforced PCL Biocomposites for Rigid Packaging. *Molecules* **2025**, *30*, 857-886.
17. Simonini, L.; Canale, R.; Mahmood, H.; Dorigato, A.; Pegoretti, A. Multifunctional epoxy/carbon composites with a fully reparable interface. *Polymer Composites* **2024**, *45*, 2558-1568.
18. Simonini, L.; Kakkonen, M.; Dsouza, R.; Kanerva, M.; Mahmood, H.; Dorigato, A.; Pegoretti, A. Tailoring the interfacial properties of glass fiber-epoxy microcomposites through the development of a self-healing poly (ϵ-caprolactone) coating. *Composites Science and Technology* **2024**, *261*, 110991-111007.
19. Simonini, L.; Mahmood, H.; Dorigato, A.; Pegoretti, A. Evaluation of self-healing capability of a polycaprolactone interphase in epoxy/glass composites. *Composites Part A: Applied Science and Manufacturing* **2023**, *169*, 107539-107548.
20. Dorigato, A.; Rigotti, D.; Pegoretti, A. Novel poly(caprolactone)/epoxy blends by additive manufacturing *Materials* **2020**, *13*, 819-826.
21. Cescato, R.; Rigotti, D.; Mahmood, H.; Dorigato, A.; Pegoretti, A. Thermal mending of electroactive carbon/epoxy laminates using a porous poly(ε-caprolactone) electrospun mesh. *Polymers* **2021**, *13*, 2723-2734.
22. Archer, E.; Torretti, M.; Madbouly, S. Biodegradable polycaprolactone (PCL) based polymer and composites. *Physical Sciences Reviews* **2023**, *8*, 4391-4414.
23. Luna, C.; Siqueira, D.; Ferreira, E.; Araujo, E.; Wellen, R. Effect of injection parameters on the thermal, mechanical and thermomechanical properties of polycaprolactone (PCL). *Journal of Elastomers and Plastics* **2021**, *53*, 1045-1062.
24. Wu, F.; Misra, M.; Mohanty, A. Challenges and new opportunities on barrier performance of biodegradable polymers for sustainable packaging. *Progress in Polymer Science* **2021**, 101395-101435.

 doi:10.20944/preprints202505.0930.v1

25. Dybka-Stępień, K.; Antolak, H.; Kmiotek, M.; Piechota, D.; Koziróg, A. Disposable food packaging and serving materials - Trends and biodegradability. *Polymers* **2021**, *19*, 3606-3644.
26. Bezerra, E.; França, D.; Morais, D.; Rosa, M.; Morais, J.; Araújo, E.; Wellen, R. Processing and properties of PCL/cotton linter compounds. *Materials Research* **2017**, *20*, 317-325.
27. Rytlewski, P.; Stepczyńska, M.; Moraczewski, K.; Malinowski, R.; Jagodziński, B.; Żenkiewicz, M. Mechanical properties and biodegradability of flax fiber-reinforced composite of polylactide and polycaprolactone. *Polimery* **2018**, *63*, 603-610.
28. Dhakal, H.; Ismail, S.; Zhang, Z.; Barber, A.; Welsh, E.; Maigret, J.; Beaugrand, J. Development of sustainable biodegradable lignocellulosic hemp fiber/polycaprolactone biocomposites for light weight applications. *Composites Part A: Applied Science and Manufacturing* **2018**, *113*, 350-358.
29. Ilyas, R.; Zuhri, M.; Norrrahim, M.; Misenan, M.; Jenol, M.; Samsudin, S.; Nurazzi, N.; Asyraf, M.; Supian, A.; Bangar, S.; R, N. Natural fiber-reinforced polycaprolactone green and hybrid biocomposites for various advanced applications. *Polymers* **2022**, *14*, 182-210.
30. Jian, B.; Mohrmann, S.; Li, H.; Li, Y.; Ashraf, M.; Zhou, J.; Zheng, X. A review on flexural properties of wood-plastic composites. *Polymers* **2022**, *14*, 3942-3961.
31. Cintra, S.; Braga, N.; Morgado, G.; Montanheiro, T.; Marini, J.; Passador, F.; Montagna, L. Development of new biodegradable composites materials from polycaprolactone and wood flour. *Wood Material Science and Engineering* **2022**, *17*, 586-597.
32. Herrera, N.; Olsen, P.; Berglund, L. Strongly improved mechanical properties of thermoplastic biocomposites by PCL grafting inside holocellulose wood fibers. *ACS Sustainable Chemistry & Engineering* **2020**, *20*, 11977-11985.
33. Lo Re, G.; Spinella, S.; Boujemaoui, A.; Vilaseca, F.; Larsson, P.; Adaš, F.; Berglund, L. Poly (ε-caprolactone) biocomposites based on acetylated cellulose fibers and wet compounding for improved mechanical performance. *ACS Sustainable Chemistry & Engineering* **2018**, *6*, 6753-6760.
34. Mohammed, M.; Rahman, R.; Mohammed, A.; Adam, T.; Betar, B.; Osman, A.; Dahham, O. Surface treatment to improve water repellence and compatibility of natural fiber with polymer matrix: Recent advancement. *Polymer testing* **2022**, *115*, 107707-107732.
35. Mahmood, H.; Simonini, L.; Dorigato, A.; Pegoretti, A. Graphene deposition on glass fibers by triboelectrification. *Applied Sciences* **2021**, *11*, 3123-3134.
36. Pozueco, S.; Simonini, L.; Mahmood, H.; Rigotti, D.; Kakkonen, M.; Riveiro, A.; Comesaña, R.; Pou, J.; Tanhuanpää, O.; Kanerva, O.; Sarlin, E.; Kallio, P.; Pegoretti, A. Influence of CO_2 laser surface treatment of basalt fibers on the mechanical properties of epoxy/basalt composites. *Polymer Composites* **2024**, *In press*.
37. Simonini, L.; Mahmood, H.; Dorigato, A.; Pegoretti, A. Tailoring the physical properties of poly (lactic acid) through the addition of thermoplastic polyurethane and functionalized short carbon fibers. *Polymer Composites* **2023**, *44*, 4719-4733.
38. Show, P.; Oladele, K.; Siew, Q.; Aziz Zakry, F.; Lan, J.; Ling, T. Overview of citric acid production from Aspergillus niger. *Frontiers in life science* **2015**, *8*, 271-283.
39. Sorze, A.; Valentini, F.; Mucignat, M.; Pegoretti, A.; A, D. Multifunctional xanthan gum/wood fibers based hydrogels as novel topsoil covers for forestry and agricultural applications. . *Carbohydrate Polymer Technologies and Applications* **2024**, *7*, 100520-100530.
40. Behera, B.; Mishra, R.; Mohapatra, S. Microbial citric acid: Production, properties, application, and future perspectives. *Food Frontiers* **2021**, *2*, 62-76.
41. Huang, F.; Tian, Z.; Wang, Y.; Ji, X.; Wang, D.; Fatehi, P. ellulose fiber drainage improvement via citric acid crosslinking. *International Journal of Biological Macromolecules* **2024**, *281*, 136338-136347.
42. Cui, X.; Ozaki, A.; Asoh, T.; Uyama, H. Cellulose modified by citric acid reinforced Poly (lactic acid) resin as fillers. *Polymer Degradation and Stability* **2020**, *175*, 109118-109125.
43. Sorze, A.; Valentini, F.; Smolar, J.; Logar, J.; Pegoretti, A.; Dorigato, A. Effect of different cellulose fillers on the properties of xanthan-based composites for soil conditioning applications. *Materials* **2023**, *16*, 7285-7305.
44. Wu, Q.; Jiang, K.; Wang, Y.; Chen, Y.; Fan, D. Cross-linked peach gum polysaccharide adhesive by citric acid to produce a fully bio-based wood fiber composite with high strength. *International Journal of Biological Macromolecules* **2023**, *253*, 127514-127523.

 doi:10.20944/preprints202505.0930.v1

45. Gebke, S.; Thümmler, K.; Sonnier, R.; Tech, S.; Wagenführ, A.; Fischer, S. Flame retardancy of wood fiber materials using phosphorus-modified wheat starch. *Molecules* **2020**, *25*, 335-356.
46. Zakaria, R.; Bawon, P.; Lee, S.; Salim, S.; Lum, W.; Al-Edrus, S.; Ibrahim, Z. Properties of particleboard from oil palm biomasses bonded with citric acid and tapioca starch. *Polymers* **2021**, *13*, 3494-3509.
47. Fu, H.; Dun, M.; Chen, B.; Zhou, Z.; Wang, H.; Wang, W.; Xie, Y.; Wang, Q. Compression rheological behavior of ultrahighly filled wood flour-polyethylene composites. . *Composites Part B: Engineering* **2021**, *215*, 108766-108781.
48. Olonisakin, K.; Lin, H.; Haojin, P.; Aishi, W.; Wang, H.; Li, R.; Xin-Xiang, Z.; W, Y. Fiber treatment impact on toughness and interfacial bonding in epoxidized soya bean oil compatibilized PLA/PBAT bamboo fiber composites. *Materials Today Communications* **2024**, *38*, 107790-107803.
49. Arman, N.; Chen, R.; Ahmad, S. Review of state-of-the-art studies on the water absorption capacity of agricultural fiber-reinforced polymer composites for sustainable construction. *Construction and Building Materials* **2021**, *302*, 124174-124188.
50. Sekar, S.; Suresh Kumar, S.; Vigneshwaran, S.; Velmurugan, G. Evaluation of mechanical and water absorption behavior of natural fiber-reinforced hybrid biocomposites. *Journal of Natural Fibers* **2022**, *19*, 1772-1782.
51. Arul, S.; Adhikary, P.; SiP, J.; Haiter Lenin, A. Moisture diffusion analysis and their effects on the mechanical properties of organic particle filled natural fiber reinforced hybrid polymer composites. *International Journal of Polymer Analysis and Characterization* **2024**, *29*, 42-55.
52. Khorramnezhad, M.; Akbari, B.; Akbari, M.; Kharaziha, M. Effect of surface modification on physical and cellular properties of PCL thin film. *Colloids and Surfaces B: Biointerfaces* **2021**, *200*, 111582-111589.
53. Ruiz, M.; Martin, J.; Celada, L.; Olsén, P.; Wågberg, L. Strategic functionalization of wood fibers for the circular design of fiber-reinforced hydrogel composites. *Cell Reports Physical Science* **2025**, *1*, 1-15.